

ARTICLES

Temperature Dependence of Local Density Augmentation for Acetophenone *N,N,N',N'*-Tetramethylbenzidine Exciplex in Supercritical Water**Takafumi Aizawa,^{*,†} Mitsuhiro Kanakubo,[†] Yusuke Hiejima,[†] Yutaka Ikushima,[†] and Richard L. Smith, Jr.[‡]**

Compact Chemical Process Research Center, National Institute of Advanced Industrial Science and Technology, 4-2-1 Nigatake, Miyagino-ku, Sendai 983-8551, Japan, and Graduate School of Chemical Engineering, Research Center of Supercritical Fluid Technology, Tohoku University, Aoba 07, Aramaki-Aza, Aoba-ku, Sendai 980-8579, Japan

Received: March 16, 2005; In Final Form: June 22, 2005

Local density augmentation around exciplex between acetophenone and *N,N,N',N'*-tetramethylbenzidine in supercritical water was measured by observing the peak shift of transient absorption spectrum at temperatures from 380 to 410 °C and at pressures from 6 to 37 MPa. Large local density augmentation was observed at lower solvent densities. Local density augmentation was evaluated by the excess density, which was defined as the difference between local density and bulk density, and the density enhancement factor, which was defined by the ratio of the local density to the bulk density. The number of solvating molecules was estimated with a Langmuir adsorption model. The excess density was found to exhibit a maximum at approximately 0.15 g cm⁻³, which decreased with increasing temperature. The density enhancement factor was found to decrease with increasing temperature; however, its value was much greater than unity at 410 °C, which provides evidence that exciplex–water interactions still exist at these conditions. The temperature dependence of local density augmentation around the exciplex in supercritical water was comparable with that in supercritical carbon dioxide, which suggests that the ratios of the solute–solvent and solvent–solvent interactions are comparable between these two systems.

1. Introduction

The presence of density inhomogeneities in both pure fluids and solutions is a characteristic feature of fluids near their critical point.^{1–5} Nishikawa et al. evaluated density fluctuations in pure carbon dioxide^{1,2} and pure water³ by small-angle X-ray scattering. The density fluctuations became large and reached a maximum near the critical density.^{4,5} In dilute supercritical solutions, local density augmentation around solute molecules has been observed,⁶ and the phenomena has been shown to be due to short-range interactions between the solute and the solvent.^{7,8} Local density augmentation should play an important role in specific chemical reactions in supercritical fluids and in understanding phenomena such as high-selectivity reactions⁹ and high-speed reactions.¹⁰ Since local density augmentation is a result of short-range interactions, it has been actively researched by observing probe molecules with spectroscopic methods such as NMR,¹¹ UV/Vis,¹² electron paramagnetic resonance,¹³ and fluorescence¹⁴ spectroscopy. In previous work, we clarified the local density augmentation that occurs around transient species with a time-resolved method.^{15–17}

Most studies on local density augmentation have focused on supercritical carbon dioxide or other supercritical fluids for which the critical temperature is not too high. There have been few studies on water in its supercritical state, because of the

difficulty in performing spectroscopic measurements at high-pressure and high-temperature conditions. However, previous studies^{18,19} that have examined local density augmentation around long-lived species in supercritical water have found that weak local density augmentation still exist at elevated temperatures (>647 K) and high pressures (>22.1 MPa). Since the characteristics of the short-lived species, such as reaction intermediates, are key to elucidating the underlying chemical reaction mechanisms, evaluation of local density augmentation around short-lived species should be important in processes such as formation of radicals, ionic species, or molecular rearrangements. In a previous study,²⁰ we determined the local density augmentation around exciplex, a short-lived species, in supercritical water at a constant temperature of 380 °C and found that local density augmentation exists in the low-pressure (6–25 MPa) region. The temperature dependence of local density augmentation around exciplex needs to be clarified as the next step in our investigation.

In this paper, we report on the temperature and pressure dependence of the peak positions of exciplex in supercritical water by a transient absorption technique and estimate the temperature dependence of the local density augmentation around transient species in supercritical water. Since short-range interactions affect the UV/Vis absorption spectra, peak shift analyses were carried out and used to analyze the microscopic structure around probe molecules so that comparisons could be made with other literature results.^{21–23} Exciplex between acetophenone (AP) and *N,N,N',N'*-tetramethylbenzidine (TMB)

* To whom correspondence should be addressed. E-mail: t.aizawa@aist.go.jp.

[†] National Institute of Advanced Industrial Science and Technology.

[‡] Tohoku University.

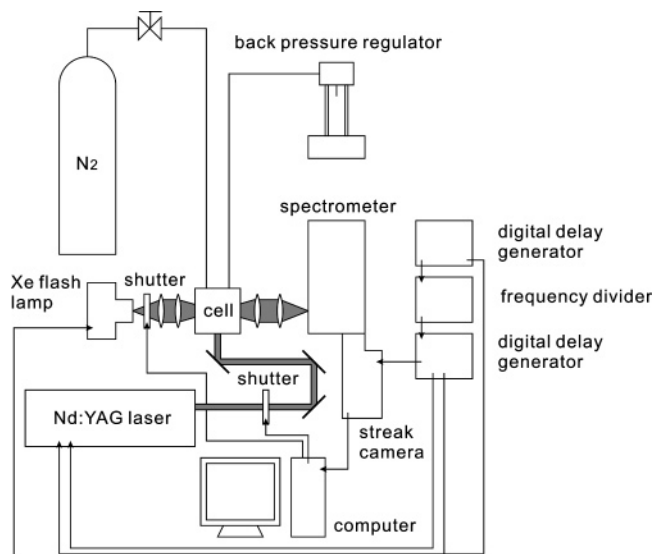


Figure 1. Schematic diagram of the transient absorption apparatus.

was chosen as a target species because this reaction and local density augmentation have been studied by our group at 380 °C.

2. Experimental Section

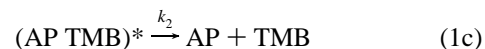
A high-pressure high-temperature transient absorption technique was used to observe UV/Vis absorption of reaction intermediates.²⁰ A schematic diagram of the apparatus is shown in Figure 1. The light source and timing generator of the transient absorption measurement system were the same as in the previous study²⁴ and consisted of a spectrometer (Hamamatsu Photonics C5094), a Nd:YAG laser (Spectra-Physics GCR-130; 355 nm; 90 mJ; pulse width 5–6 ns) as an excitation source, a Xe flash lamp (Tokyo Instruments XF-80; 60 W) as a monitoring source, two digital delay generators (Stanford Research DG-535) and a simple frequency divider as a digital

delay line, and the optical cell. The frequency divider was used to reduce repetition time to 2.5 Hz, which was caused by the limitation of Xe flash lamp (<3 Hz). A high-sensitivity, high-dynamic range streak camera (Hamamatsu Photonics C7700) was used as the detector. A cross-sectional diagram of the high-temperature high-pressure optical cell is shown in Figure 2. The cell was custom designed for the experiments considered in this work and consisted of antisymmetrically placed windows, commercially available high-temperature seals (Taiatsu Techno, TTS seal, Tokyo), and a double-window system that used sapphire and quartz as described in our previous paper.²⁰ One port of the cell was connected to a nitrogen gas cylinder, and the other port was connected to a back-pressure regulator. The pressure was monitored by the pressure gauge of the back-pressure regulator.

AP and TMB purchased from Tokyo Pure Chemical Industries were used without further purification. Sample concentrations were 5×10^{-2} and 5×10^{-4} M for AP and TMB, respectively. Measurements were performed with the following procedure. A certain amount of AP and TMB was put into the cell at atmospheric conditions. After water was loaded, nitrogen gas was flowed through the cell for 120 s to purge the air. The cell was heated from the given temperature from room temperature in 30 min; however, another 30 min was required for stabilization, so that measurements were initiated 60 min after the initial heating.

3. Results and Discussion

The reaction scheme of AP–TMB system can be described according to the literature²⁵ as follows



When AP is irradiated with Nd:YAG laser light at 355 nm, it

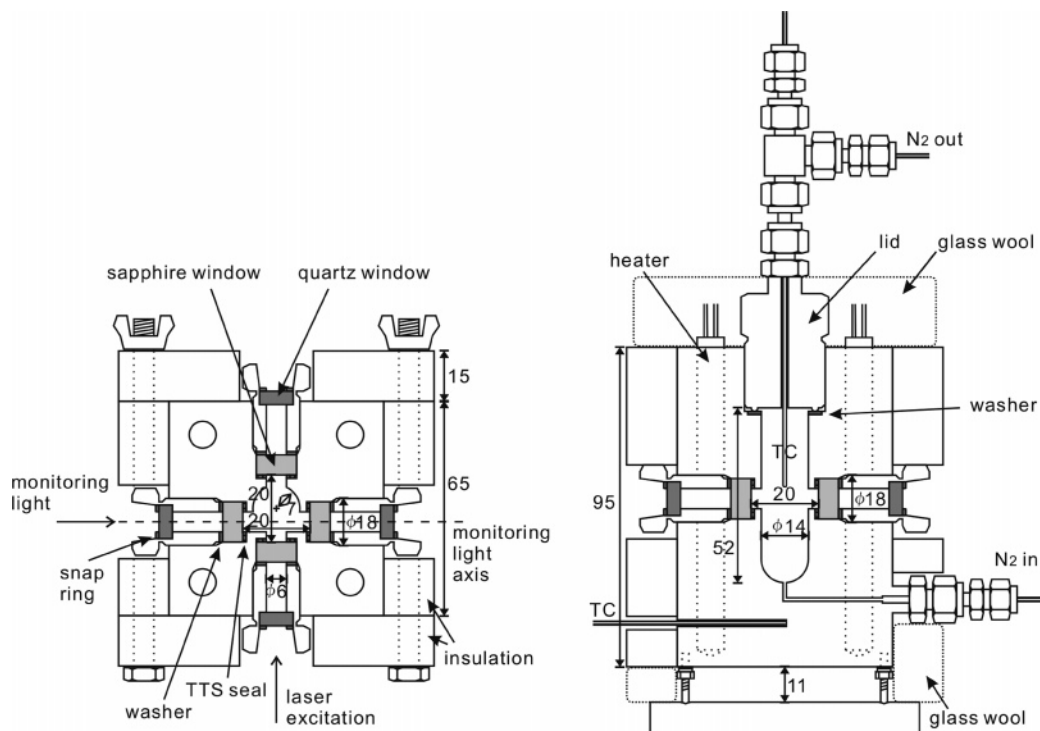


Figure 2. Horizontal (left) and vertical (right) cross section of the cell. Light shading: sapphire windows. Dark-gray shading: quartz windows.

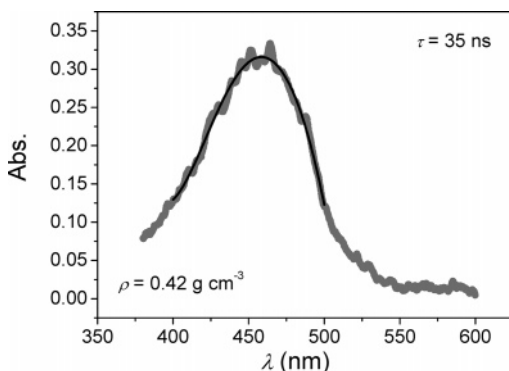


Figure 3. Absorption spectrum of the exciplex AP-TMB system at 380 °C and 0.42 g cm⁻³ at 35 ns after laser flash. The black solid line is a polynomial fit to the data.

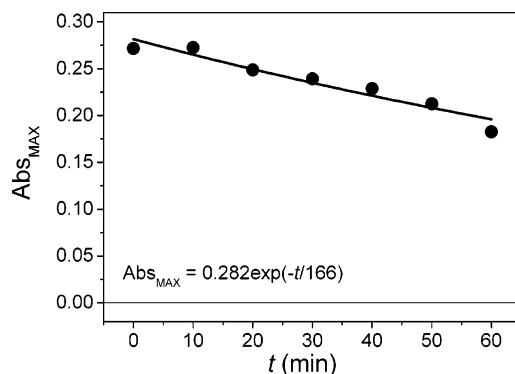


Figure 4. Decay of absorption intensity at 380 °C at 0.45 g cm⁻³. The decay rate is $6.0 \times 10^{-3} \text{ min}^{-1}$ and was caused by sample decomposition.

is brought to an excited state (AP*). The AP* is highly reactive toward TMB and forms an exciplex (AP-TMB)*, which subsequently undergoes decay. The reaction intermediate is an exciplex, which has absorption at around 450 nm (Figure 3).

Peak position of the exciplex did not differ so much compared with our previous results in supercritical carbon dioxide.^{15,16} It is difficult to obtain peak position from experimental data directly, because of the noise in the spectrum. Therefore, the spectrum was fit with a sixth-order polynomial from 400 to 500 nm, and the peak position was derived by the peak position of the fitted polynomial. This procedure was almost the same as that used in our previous study.²⁰

The decomposition of the compounds was estimated by the time dependence of the exciplex signal and was almost 30% over the 60-min time period at 380 °C (Figure 4). In this work, we used peak position in the analyses, and so peak intensity caused by slight decomposition was of lesser importance.

The density dependence of peak position is shown in Figure 5. Density was calculated from the system temperature and pressure with the PROPATH program²⁶ that is based on IUPAC recommended rules. Each point was obtained by different experiments, and further, at 380 °C, experimental data were measured from low density to high density and from high density to low density, alternately, to help avoid systematic errors. Since the experimental results exhibited a continuous curve, it was concluded that the peak positions could be determined with sufficient accuracy. The data obtained at densities greater 0.45 g cm⁻³ exhibited linearity; however, deviation from linearity was apparent in the low-density region from 0.05 to 0.35 g cm⁻³. This type of plot is sometimes used in spectroscopic studies¹² for demonstrating the existence of local density augmentation in supercritical fluids. From the PVT

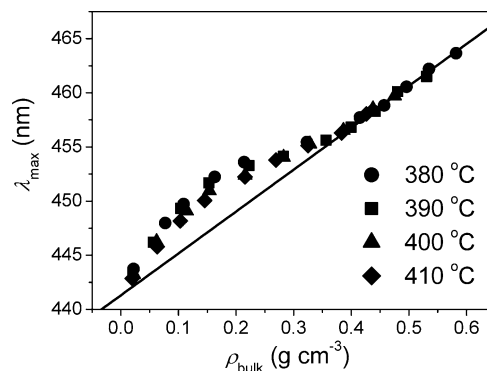


Figure 5. Density dependence of peak position of AP-TMB exciplex. Circles are experimental data. Solid line was determined from experimental data at densities greater than 0.45 g cm⁻³ by least-squares method.

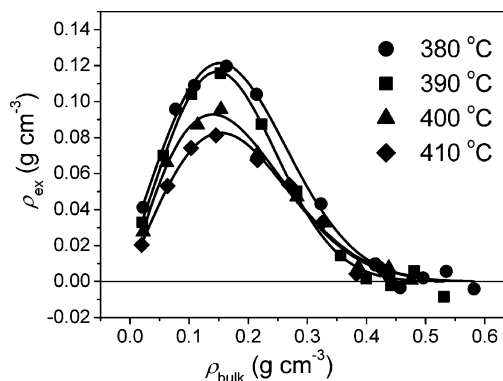


Figure 6. Excess density around exciplex at various temperatures and densities. Markers are experimental data. Solid lines are fitted Weibull functions.

data, the solid line in Figure 5 could be determined over a density range from 0.45 to 0.6 g cm⁻³ at 380 °C according to

$$\lambda_{\max} = c_1 + c_2\rho \quad (1)$$

where c_1 and c_2 are fitting parameters. The lower-density experimental data did not conform to linear behavior, and this is attributed to local density augmentation. In previous long-lived species studies,¹⁹ local density augmentation disappeared at 400 °C. In the results reported in this study, local density augmentation was found to exist for a short-lived exciplex species in supercritical water, even at higher temperatures.

The local density around exciplex, ρ_{local} , can be calculated from the experimental data and eq 1. To evaluate the local density augmentation, the excess density, ρ_{ex} , defined by the difference between the local density ρ_{local} and the bulk density ρ_{bulk} , was calculated. The derived excess density is shown in Figure 6, in which the solid line is the fitting result with a Weibull function²⁷ as follows

$$\Delta\rho = a\left(\frac{c-1}{c}\right)^{(1-c)c} \left[\frac{\rho - \rho_0}{b} + \left(\frac{c-1}{c}\right)^{1/c} \right]^{c-1} \times \exp\left\{ -\left[\frac{\rho - \rho_0}{b} + \left(\frac{c-1}{c}\right)^{1/c} \right]^c + \frac{c-1}{c} \right\} \quad (2)$$

where a , b , c , and ρ_0 are fitting parameters. ρ_0 indicates the bulk density at maximum excess density. The maximum excess density and bulk density at that time is shown in Table 1. The maximum excess density decreased with increasing temperature; however, local density augmentation still existed at 410 °C, which is probably due to strong solute-solvent interactions.

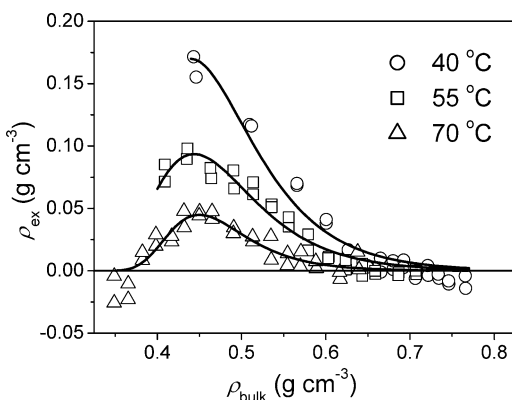


Figure 7. Excess density around exciplex at various temperatures and densities in supercritical carbon dioxide.¹⁶ Markers are experimental data. Solid lines are fitted Weibull functions.

TABLE 1: Maximum Excess Density and Bulk Density at Maximum Excess Density Determined by Weibull Fitting (Figure 6)

| T (°C) | maximum excess density (g cm^{-3}) | bulk density at maximum excess density (g cm^{-3}) |
|----------|---|---|
| 380 | 0.121 | 0.152 |
| 390 | 0.117 | 0.147 |
| 400 | 0.093 | 0.140 |
| 410 | 0.083 | 0.154 |

Excess density exhibited a maximum at almost 0.15 g cm^{-3} for most temperatures in which conditions of density were much lower than the critical density of water that is 0.32 g cm^{-3} . The phenomenon of the maximum at low bulk density is also observed for anthracene in supercritical carbon dioxide.²⁸ The lower peak position is affected by solute–solvent interactions,¹⁸ so it is probable that the AP–TMB exciplex had strong interactions with water molecules. Compared with 4-nitroaniline¹⁸ in supercritical water, the bulk density at maximum excess density was lower, which also suggests strong solute–solvent interactions. The strong solute–solvent interactions should be caused by the large dipole moment of the exciplex, which has positive and negative partial charges. According to previous results,¹⁹ local density augmentation is not expected to be as large in supercritical water and should disappear rapidly with an increase of temperature because of solvent–solvent interactions of the aqueous environment. However, our results show the possibility that local density augmentation still exists at 410 °C and strong solute–solvent interactions are still present in this exciplex system.

Comparison with our previous results in carbon dioxide was carried out. Figure 7 shows the excess density around the AP–TMB exciplex in carbon dioxide.¹⁶ Solid lines are derived by Weibull function fitting. Figure 8 shows the temperature dependence of the excess density as derived by Weibull fitting. Density and temperature were scaled by division of the critical density ρ_c and critical temperature T_c , respectively, for each substance, carbon dioxide and water. From Figure 8, the decrease in local density augmentation with temperature was almost the same for both supercritical carbon dioxide and supercritical water. The local density augmentation was determined by the ratio between solute–solvent and solvent–solvent interactions. Our results show that the ratios of the solute–solvent and solvent–solvent interactions are comparable between these two systems as discussed in a later section.

If we assume that the local density augmentation can be described by a Langmuir adsorption model,²⁹ the local density

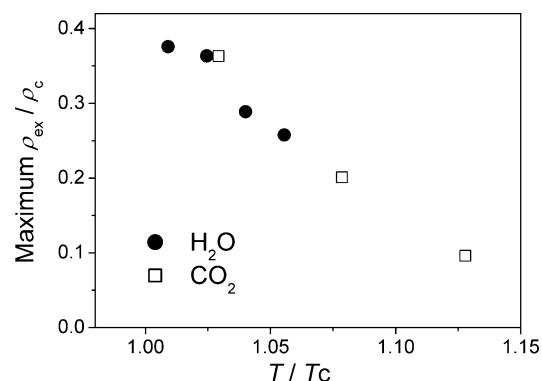


Figure 8. Temperature dependence of maximum excess density around exciplex in supercritical carbon dioxide¹⁶ and supercritical water.

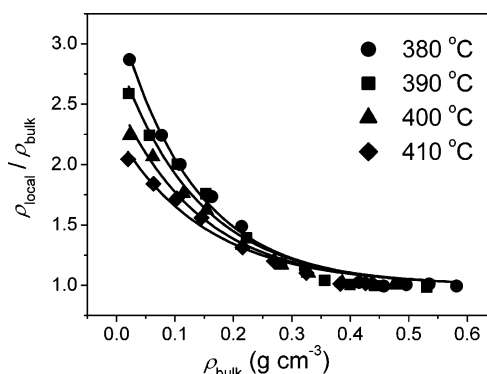


Figure 9. Density enhancement factor at various temperatures and densities. Markers are experimental data. Solid lines are fitted by eq 3.

TABLE 2: Density Enhancement Factor at $\rho_{\text{bulk}} = 0$ (Value Established by the Fitting of Figure 8)

| T (°C) | density enhancement factor ($d_1 + 1$) |
|----------|--|
| 380 | 3.26 |
| 390 | 2.91 |
| 400 | 2.55 |
| 410 | 2.25 |

can be roughly evaluated by the density enhancement factor defined $\rho_{\text{local}}/\rho_{\text{bulk}}$ ²⁸ that monotonically decreases with increasing ρ_{bulk} .^{30–32} The density enhancement factor of AP–TMB exciplex is shown in Figure 9. The solid line was fitted by single-exponential decay function as follows

$$\rho_{\text{local}}/\rho_{\text{bulk}} = 1 + d_1 \exp(-d_2 \rho_{\text{bulk}}) \quad (3)$$

where d_1 and d_2 are fitting parameters. The value $(d_1 + 1)$ indicates the strength of solute–solvent interactions compared with solvent–solvent interactions and is denoted as the density enhancement factor. The density enhancement factor for each temperature is shown in Table 2, where its value of 3.3 at 380 °C was comparable to the value reported in anthracene in supercritical carbon dioxide²⁸ that also exhibits strong solute–solvent interactions. It is sometimes said that local density augmentation should not be as large in supercritical water compared with that in supercritical carbon dioxide because of the strong solvent–solvent interaction in the aqueous environment. However, our results show that a similar degree of local density augmentation exists for reaction systems in supercritical water as demonstrated by our measurements on short-lived species. The strong solute–solvent interaction can be understood by high polarity of exciplex that probably attracts water molecules.

In the context of this discussion, it is necessary to define strong solute–solvent interactions. Our results show similar degrees of local density augmentation for short-lived species in both supercritical carbon dioxide and in supercritical water. For both of these cases, the meaning of strong solute–solvent interactions might seem to be similar. However, the degree of local density augmentation should be estimated by considering solute–solvent interactions *relative* to solvent–solvent interactions. The absolute value of interactions between exciplex and carbon dioxide molecules should be weaker than that between exciplex and water molecules, because carbon dioxide has no dipole moment and further because the partial charge on carbon and oxygen atoms are smaller compared with the water molecule. However, the ratios of solute–solvent and solvent–solvent interactions are probably comparable between these two systems, which is probably because ratios of weak interactions are present in carbon dioxide and ratios of strong interactions are present in water. Since the solvent–solvent interaction between carbon dioxide molecules is weak, the weak solute–solvent interaction must cause large local density augmentation. On the other hand, it was expected that interactions between polar molecules and water molecule should be high. However, the water molecules have a strong hydrogen-bond network, and it can be reasoned that this hydrogen network provides a barrier to the formation of a large local density augmentation. From other results in the literature, it has been determined by Raman³³ and NMR³⁴ spectroscopy that hydrogen bonds still exist in water at high temperatures and pressures but that the hydrogen-bond network is greatly weakened above the critical temperature. Oka and Kajimoto said that the position of maximum excess density was most likely related to the solute–solvent and solvent–solvent interactions.¹² Strong solute–solvent interactions seemed to make the peak position lower, which is consistent with our observations. Furthermore, those authors suggested that for cases of strong solute–solvent interactions, the local density augmentation would probably occur over wide ranges of bulk density. According to the findings reported in this work and those in the literature, if the solute–solvent interactions are weaker than the solvent–solvent interactions, one might expect that the local density augmentation might only be observable near the critical point. Further, if the solute–solvent interactions are larger than solvent–solvent interactions, local density augmentation is most likely observable over wide ranges of temperature and pressure (or density). The results reported in this study are direct evidence of latter case. In our exciplex system, local density augmentation could be observed over a wide range of temperatures compared with the previous results obtained for the 4-nitroaniline systems, which suggests that the exciplex–water interactions are much stronger than in the 4-nitroaniline–water interactions relative to the respective solvent–solvent interactions. In an attempt to understand the local density augmentation between these various systems, exciplex dipole moments were estimated. The AP–TMB exciplex has a large dipole moment of 17 D that was estimated in supercritical carbon dioxide.¹⁵ On the other hand, the dipole moment of 4-nitroaniline was evaluated to be 7 D that was calculated by MOPAC 6. Species that have large dipole moments should be more strongly attracted to water molecules. The higher polarity of the AP–TMB exciplex over that of 4-nitroaniline might be one of the reasons for the large local density augmentation that was observed for the AP–TMB exciplex in supercritical water.

Detailed Langmuir adsorption model analyses were carried out to estimate the number of solvating molecules around

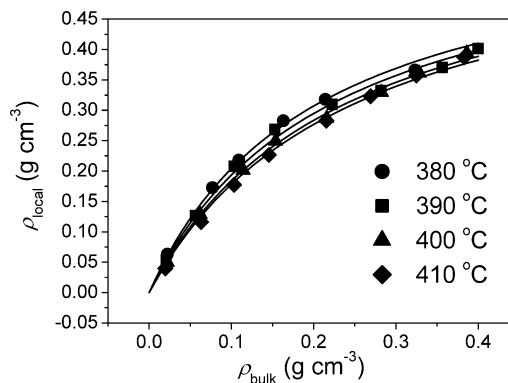


Figure 10. Langmuir adsorption model fitted to data at various temperatures and densities. Markers are experimental data. Solid lines were determined from eq 6.

TABLE 3: Parameters of Langmuir Adsorption Model Established by the Fitting of Figure 10

| T (°C) | ρ_1 (g cm ⁻³) |
|----------|--------------------------------|
| 380 | 0.00231 |
| 390 | 0.00250 |
| 400 | 0.00269 |
| 410 | 0.00281 |

exciplex. The Langmuir adsorption model derived by Kajimoto et al.²⁹ was shown as follows

$$n = \frac{n_{\max} \rho_{\text{bulk}}}{\rho_1 (n_{\max} - 1) + \rho_{\text{bulk}}}, \quad (4)$$

where n is the number of solvating molecules around a solute, n_{\max} is the maximum number of the solvating molecules, and ρ_1 is the bulk density of the solvent corresponding to $n = 1$. ρ_{local} was related to n by the factor f by the following equation

$$\rho_{\text{local}} = fn \quad (5)$$

Finally, the experimental results in this work were fitted by

$$\rho_{\text{local}} = f \frac{n_{\max} \rho_{\text{bulk}}}{\rho_1 (n_{\max} - 1) + \rho_{\text{bulk}}} \quad (6)$$

where f , n_{\max} , and ρ_1 are fitting parameters. Initially, f , n_{\max} , and ρ_1 were determined at each temperature with a least-squares method. Then, f and n_{\max} were determined by averaging all temperatures, in which f and n_{\max} were determined to be 89.1 and 0.00695 g cm⁻³, respectively. Finally, ρ_1 was determined by the fitting at fixed f and n_{\max} . All fitting was performed for data where local augmentation occurred ($\rho_{\text{bulk}} < 0.4$ g cm⁻³). Fitting results are shown in Figure 10 and Table 3. The derived n_{\max} (89.1) value is quite high compared with the value described in ref 12; however, this can be attributed to the large size of the molecule forming the exciplex. By assumption that the exciplex radius is almost the same as TMB and by use of $r_{\text{ex}} = 0.65$ nm³⁵ and a radius for water as $r_{\text{water}} = 0.145$ nm, the n_{\max} was determined to be equal to 94.4 from the following equation¹²

$$n_{\max} = 4\pi(r_{\text{ex}} + r_{\text{water}})^2 / (2r_{\text{water}})^2 \quad (7)$$

From Figure 9, it can be seen that the local density augmentation could be well described by the Langmuir adsorption model. From the fitting results and eq 4, the number of the solvating molecules around the exciplex was calculated as shown in Figure 11. The number of solvating molecules increased more than that predicted by increasing bulk density. It has been suggested

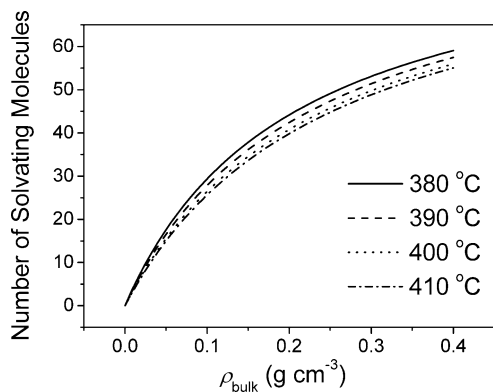


Figure 11. Number of solvating molecules around the AP–TMB exciplex in water at various temperatures and densities.

the possibility of enhancement in water-participating reactions, such as hydrolysis, if polar intermediates are generated.

4. Conclusions

In summary, temperature dependence of local density augmentation for the AP–TMB exciplex was evaluated by transient absorption measurements. Analysis of data with excess density and density enhancement factor allowed estimation of the local density augmentation. The number of solvating molecules could be estimated with a Langmuir adsorption model. Local density augmentation was found to decrease with increasing temperature. However, local density augmentation was found to exist in water at temperatures as high as 410 °C, which suggests strong solute–solvent interactions. Excess density showed a maximum at a density of around 0.15 g cm⁻³. The peak of the excess density at lower bulk densities also provides further evidence of strong solute–solvent interactions. The strong solute–solvent interactions are probably due to the high polarity of the exciplex and its attraction for surrounding water molecules. The local density augmentation of our exciplex system showed a similar tendency in both carbon dioxide and water, which suggests the ratio between solute–solvent interactions and solute–solute interactions is comparable in this system. It can be concluded that strong local density augmentation can be expected for polar solutes, even for supercritical water.

Acknowledgment. This research was partially supported by Industrial Technology Research Grant Program in '03 from New Energy and Industrial Technology Development Organization of Japan.

References and Notes

- (1) Nishikawa, K.; Tanaka, I. *Chem. Phys. Lett.* **1995**, *244*, 149–152.
- (2) Nishikawa, K.; Tanaka, I.; Amemiya, Y. *J. Phys. Chem.* **1996**, *100*, 418–421.
- (3) Morita, T.; Kusano, K.; Ochiai, H.; Saitow, K.; Nishikawa, K. *J. Chem. Phys.* **2000**, *112*, 4203–4211.
- (4) Tucker, S. C. *Chem. Rev.* **1999**, *99*, 391–418.
- (5) Goodyear, G.; Maddox, M. W.; Tucker, S. C. *J. Phys. Chem. B* **2000**, *104*, 6258–6265.
- (6) Kajimoto, O. *Chem. Rev.* **1999**, *99*, 355–389.
- (7) Tucker, S. C.; Maddox, M. W. *J. Phys. Chem. B* **1998**, *96*, 2437–2453.
- (8) Saitow, K.; Nakayama, H.; Ishii, K.; Nishikawa, K. *J. Phys. Chem. A* **2004**, *108*, 5770–5784.
- (9) Ikushima, Y.; Saito, N.; Arai, M. *J. Phys. Chem.* **1992**, *96*, 2293–2297.
- (10) Ellington, J. B.; Park, K. M.; Brennecke, J. F. *Ind. Eng. Chem. Res.* **1994**, *33*, 965–974.
- (11) Kanakubo, M.; Aizawa, T.; Kawakami, T.; Sato, O.; Ikushima, Y.; Hatakeda, K.; Saito, N. *J. Phys. Chem. B* **2000**, *104*, 2749–2758.
- (12) Otomo, J.; Koda, S. *Chem. Phys.* **1999**, *242*, 241–252.
- (13) deGrazia, J. L.; Randolph, T. W.; O'Brien, J. A. *J. Phys. Chem. A* **1998**, *102*, 1674–1681.
- (14) Khajepour, M.; Kauffman, J. F. *Chem. Phys. Lett.* **1998**, *297*, 141–146.
- (15) Aizawa, T.; Janttarakeeree, S.; Ikushima, Y.; Saitoh, N. *Chem. Phys. Lett.* **2002**, *354*, 298–302.
- (16) Aizawa, T.; Kanakubo, M.; Ikushima, Y.; Smith, R. L. *Fluid Phase Equilib.* **2004**, *219*, 37–40.
- (17) Aizawa, T.; Ikushima, Y.; Saitoh, N.; Arai, K.; Smith, R. L. *Chem. Phys. Lett.* **2002**, *357*, 168–172.
- (18) Oka, H.; Kajimoto, O. *Phys. Chem. Chem. Phys.* **2003**, *5*, 2535–2540.
- (19) Kometani, N.; Takemiya, K.; Yonezawa, Y.; Amita, F.; Kajimoto, O. *Chem. Phys. Lett.* **2004**, *394*, 85–89.
- (20) Aizawa, T.; Kanakubo, M.; Ikushima, Y.; Smith, R. L.; Saitoh, T.; Sugimoto, N. *Chem. Phys. Lett.* **2004**, *393*, 31–35.
- (21) Bulgarevich, D. S.; Sako, T.; Sugeta, T.; Otake, K.; Sato, M.; Uesugi, M.; Kato, M. *J. Chem. Phys.* **1998**, *108*, 3915–3921.
- (22) Takahashi, K.; Abe, K.; Sawamura, S.; Jonah, C. D. *Chem. Phys. Lett.* **1998**, *282*, 361–368.
- (23) Sun, Y.-P.; Fox, M. A.; Johnston, K. P. *J. Am. Chem. Soc.* **1992**, *114*, 1187–1194.
- (24) Aizawa, T.; Kanakubo, M.; Ikushima, Y.; Saitoh, N.; Arai, K.; Smith, R. L. *J. Supercrit. Fluids* **2004**, *29*, 313–317.
- (25) Kavarnos, G. J.; Turro, N. J. *Chem. Rev.* **1986**, *86*, 401–449.
- (26) *PROPATH: A Program Package for Thermophysical Properties*, version 10.2; PROPATH Group: July 1997.
- (27) Song, W.; Biswas, R.; Maroncelli, M. *J. Phys. Chem. A* **2000**, *104*, 6924–6939.
- (28) Lewis, J. E.; Biswas, R.; Robinson, A. G.; Maroncelli, M. *J. Phys. Chem. B* **2001**, *105*, 3306–3318.
- (29) Kajimoto, O.; Futakami, M.; Kobayashi, T.; Yamasaki, K. *J. Phys. Chem.* **1988**, *92*, 1347–1352.
- (30) Carlier, C.; Randolph, T. W. *AIChE J.* **1993**, *39*, 876–884.
- (31) Zhang, J. W.; Lee L. L.; Brennecke, J. F. *J. Phys. Chem.* **1995**, *99*, 9268–9277.
- (32) Rice, J. K.; Niemeyer, E. D.; Bright, F. V. *J. Phys. Chem.* **1996**, *100*, 8499–8507.
- (33) Ikushima, Y.; Hatakeda, K.; Saito, N.; Arai, M., *J. Chem. Phys.* **1998**, *108*, 5855–5860.
- (34) Matubayasi, N.; Wakai, C.; Nakahara, M. *J. Chem. Phys.* **1998**, *107*, 9133–9140.
- (35) Ranjit, K. T.; Kevan, L. *Phys. Chem. Chem. Phys.* **2001**, *3*, 2921–2927.